Thermal Annealing Effects on the Atomic Layer Deposited LaAlO₃ Thin Films on Si Substrate

Dail Eom,[a] Cheol Seong Hwang,[a,*,z] Hyeong Joon Kim,[a,*,z] Mann-Ho Cho,[b] and K. B. Chung[c]

[a]*Department of Materials Science and Engineering, and Inter-university Semiconductor Research Center, Seoul National University, Seoul 151-744, Korea*
[b]*Institute of Physics and Applied Physics, Yonsei University, Seoul 120-749, Korea*
[c]*Department of Physics, North Carolina State University, Raleigh, North Carolina 27695-8202, USA*

The changes in film structure of amorphous atomic layer deposited LaAlO₃ thin films after thermal annealing were examined by medium-energy ion-scattering measurements and angle-resolved X-ray photoelectron spectroscopy. Thermal annealing induces Si-rich LaSiO and Al-deficient $LaAl_xSi_yO_z$ layers on a few monolayers of SiO_2. Al atoms do not participate in silicate formation during annealing. Instead, they migrate toward the film surface, which induces nonhomogeneity in the films along the vertical direction. The concentrations of Al and La on the film surface increase and decrease, respectively, as a result of Si diffusion from the substrate and silicate formation.
© 2008 The Electrochemical Society. [DOI: 10.1149/1.2916437] All rights reserved.

LaAlO₃ is a promising gate dielectric material in future complementary metal-oxide-semiconductor devices on account of its larger bandgap ($\sim$6.2 eV) and comparable dielectric constant (24–27) compared with HfO_2.[1,2] It is also thermodynamically stable on Si substrates.[3,4] It was reported that as-deposited amorphous LaAlO₃ films on Si by molecular-beam deposition do not exhibit any SiO_2 or silicate interface layer.[4] Moreover, epitaxial Si films maintain an abrupt interface with LaAlO₃ substrates even after annealing at 900°C.[3] However, the interfacial stability of LaAlO₃/Si varies according to the types of deposition techniques used for LaAlO₃ growth. In many cases, inevitable interface layer formation between the amorphous LaAlO₃ thin films and Si substrate during film deposition and postdeposition annealing (PDA) have been reported.[1,2,5-9] Interface layer formation normally has an adverse effect on the device performance. In this study, the equivalent oxide thickness of a LaAlO₃ film increased from 2.23 to 2.46 nm after PDA at 800°C. However, the mechanisms for the interfacial reaction between the LaAlO₃ thin films and Si substrate during film deposition and PDA are not completely understood. Previous studies using angle-resolved X-ray photoelectron spectroscopy (ARXPS)[1] and secondary ion mass spectroscopy[2] reported that Al-deficient interfacial $La_xAl_yO_z$Si layers are formed during film growth. The authors also reported a loss of interfacial Al atoms, which had been interposed between the La_2O_3 layer and Si substrate.[10] Moreover, an Al-rich surface layer was obtained from the La_2O_3/Al(O,N)/Si structure after thermal annealing at 800°C.[10] It was suggested that the migration of Al atoms to the surface is related to interface layer formation. In order to adopt LaAlO₃ films as a gate oxide, studies on changes in film/substrate structure and the stoichiometry of LaAlO₃ films at high temperatures are essential.

In this study, 5–6 nm thick LaAlO₃ thin films were deposited on Si substrates by the sequential deposition of La_2O_3 and Al_2O_3 sub-monolayers in an atomic layer deposition (ALD) manner. The LaAlO₃ films were annealed by rapid thermal annealing (RTA) and the structural variations were investigated.

An alternating layer of La_2O_3 and Al_2O_3 thin films were deposited on a p-type Si(100) wafer to form a LaAlO₃ film. The Si wafers were cleaned using a sulfuric-peroxide mixture cleaning (H_2SO_4:H_2O_2 = 4:1, 120°C) and subsequent dipping in a diluted HF solution (HF:H_2O = 1:100). Tris(isopropyl-cyclopentadienyl)lanthanum [La(iPrCp)₃], trimethylaluminum [Al(CH₃)₃], and water were used as the La and Al precursors and

oxidant, respectively. Air-operated valves automatically controlled the injection of the metal precursor and oxidant. The La and Al precursors were vaporized at 150°C and room temperature, respectively. The excessive source and oxidant gases were purged by Ar (600 sccm) between each precursor and H_2O injection. The chamber pressure was maintained at <0.3 Torr. The substrate temperature was varied from 176 to 380°C. PDA was performed in N_2 ambient at 800°C for 30 s using RTA.

The changes in film structure and the stoichiometry of the films were examined using medium-energy ion-scattering (MEIS) measurements. MEIS analysis was accomplished using a 100 keV proton beam in double alignment in order to reduce the contributions from the crystalline Si substrate and to allow deconvolution of the spectra into contributions from Al atoms and Si signals. The composition and chemical properties of the films were analyzed by ARXPS (Kratos, AXIS-His) using Mg Kα (1253.6 eV) X-rays with a 40 eV pass energy. The depth profiles of the samples were accomplished by chemical etching of the films using a mixed acid solution (H_3PO_4:H_3COOH:HNO_3:DI = 16:1:1:580) and X-ray photoelectron spectroscopy (XPS). This setup minimized the structural and chemical modification of the film surface compared with the case using Ar⁺ ion sputtering. It was confirmed that wet etching does not cause structural and chemical modifications of its own kind using XPS.

Figure 1a shows the MEIS spectra of the as-deposited and annealed LaAlO₃ films. The thickness of the as-deposited film was 5.7 nm, as determined by ellipsometry, which increased to 6.2 nm after PDA. In MEIS, the La peak of the annealed LaAlO₃ film showed increased peak width and decreased intensity compared with that of the as-deposited film. This indicates an increase in film thickness and a decrease in the density of La atoms. The density of films normally increases with thermal annealing. Therefore, the decrease in La density originates from the substitution of La with other elements, e.g., Al, Si, etc. The increase in intensity is notable in the Al and Si peak at an energy of approximately 89 eV after thermal annealing. This suggests an increase in the density of Al and Si atoms near the film surface. Figures 1b and c show the atomic depth profiles from a simulation of the MEIS spectra of the as-deposited and annealed films, respectively. Table I gives the areal density of each element composing the films. The relative areal density was normalized to the La content. The O to [1.5(Al + La) + 2Si] ratio shows that the as-deposited film is O-deficient. After annealing, the O content increased but the films are still slightly O-deficient due to the severe Si diffusion in the films. In the as-deposited film, the atomic concentrations of La and Al atoms were relatively constant throughout the whole film thickness, and there are no Si atoms in the LaAlO₃ film bulk. However, after annealing, the Al concentration
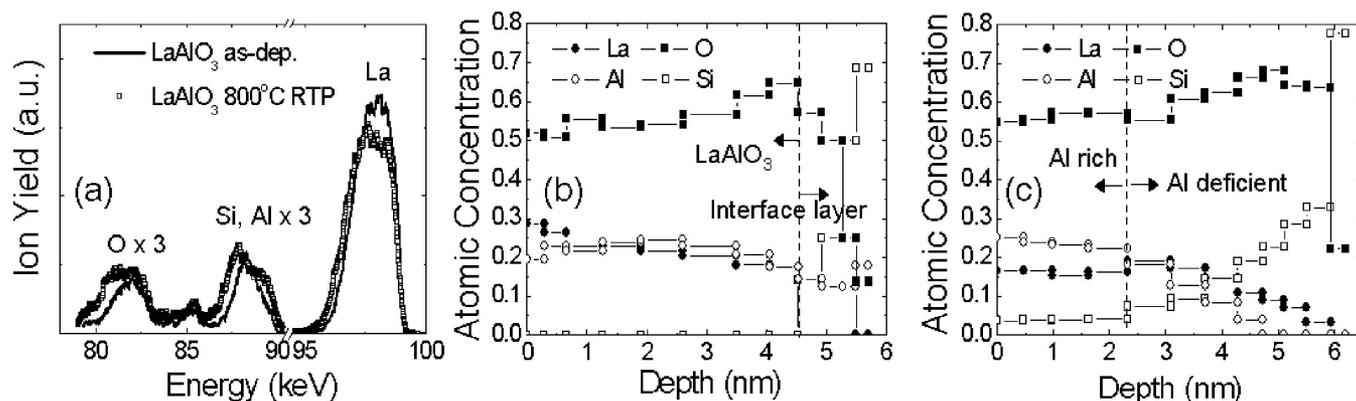
Figure 1. (a) MEIS spectra of the as-deposited and annealed film, (b) depth profile of the as-deposited film, and (c) annealed film.

increased on the film surface and decreased in the film bulk, while the La concentration showed an opposite trend, as shown in Fig. 1c. Figure 1a also shows the increases in the Si and O peak widths. The increase in the Si and O peak width is larger than that of the La peak. This was attributed to the increase in SiO_2 and Si-rich silicate interface layers. The interface layer thickness of the as-deposited film was estimated to be within a few monolayers. However, after PDA, the increases in the interface layer and Si diffusion into the $LaAlO_3$ films were significant. The surface concentration of Si on the film surface increased to ∼5%, and the Si concentration in the film bulk increased to ∼ 10%. It appears that a $(La,Al,Si)O_x$ layer had formed at the interface between the SiO_2 and surface $LaAlO_3$ layer by PDA. The boundary between the SiO_2 and La-aluminosilicate layer is unclear. The diffusion of the Si atoms and interface layer formation are accompanied by the diffusion of O atoms from the residual gas in the RTA chamber.[10,11] In Fig. 1a, the O peak area of annealed film was increased remarkably compared with that of the as-deposited film.

Figure 2 shows cross-sectional high-resolution transmission electron microscopy (HRTEM) images of the ∼ 8 nm thick (a) as-grown and (b) annealed $LaAlO_3$ film on Si substrate. They show that the layers have an amorphous structure up to an annealing temperature of 800°C. The thickness increases to 8.3 nm after annealing compared to the as-deposited film (7.7 nm). A slight increase in the interface layer is observed. However, the interfacial layer thickness is generally negligible. The image contrast between the layers composed of Al and Si atoms was not distinctive enough in these HRTEM images due to similar atomic numbers. Therefore, it seems that the decrease of Al atoms near the interface countervails the increase of Si atoms, which results in the similar contrast of the interface region.

Figures 3a-d show variations in the XPS spectra of Al 2p, La 3d, Si 2s, and O 1s peaks with decreasing film thickness by wet etching after the PDA. The inset figure in Fig. 3a shows the variations in the residual thickness and Al/(La + Al) ratio (estimated by the XPS) as a function of wet-etching time. The etch rate was ∼0.9 ± 0.1 nm/s from 0 to 3 s. After a 5 s etch, there was no further etching of the film because the remaining layer was Si-rich silicate film. The depth

profile results show the nonuniformity of the Al and La content along the depth direction, which is quite consistent with the MEIS spectra. In Fig. 3c, the peaks centered at 152–153 eV correspond to silicates.[2,10] As the etch time was increased (film thickness decreased), the peak for silicate shifts to a high binding energy (BE) from 152.2 to 153.5 eV and its intensity increases. Si atoms have higher electronegativity than La and Al atoms. Therefore the shift to higher BE with increasing etch time reveals a layer close to the Si substrate has a higher Si content.[12] The Si 2s peak of the 2.7 nm thick film is located at 153.4 eV, which is still slightly deviated from the BE of Si atoms in SiO_2 films (154.1 eV).[1] This suggests that this thin layer is still a silicate, not SiO_2. The chemical shift due to a change in composition is also shown in O 1s spectra. The BE of the O 1s spectra varies from 530.6 to 532.6 eV with decreasing film thickness. The oxygen BE before etching indicates that most O atoms are bound to La and Al atoms.[13] The BE increases with increasing etch time, suggesting that an increased amount of Si atoms had diffused into the film and bound to O atoms.

The films were also examined using ARXPS. Figure 4a shows the Al-to-La peak area ratios depending on the take-off angle of photoelectrons in the stoichiometric $LaAlO_3$ films before and after annealing. After thermal annealing, the Al/La ratio detected at a normal angle (sin θ = 1) increased from 1.0 in the as-deposited film to 1.6 in the annealed film. Because the total amount of La atoms in the $LaAlO_3$ films did not decrease after annealing at 800°C in the MEIS spectra (Table I) and X-ray fluorescence spectroscopy analysis (data not shown), the increase in the Al/La ratio showed that Al atoms had diffused up to the film surface, where more photoelectrons escape without a loss of kinetic energy than the inner part of the film, and the La atoms diffused into the film inside. After annealing, the Al/La ratio became larger at a low take-off angle (smaller sin θ value). Detection at a low take-off angle is more sensitive to the surface, and detection in the normal direction is more sensitive to the bulk and interface. Therefore, this also shows that Al atoms diffused up to the film surface by PDA. Figure 4b shows the changes in the Al/La peak area ratios of the angle-resolved X-ray photoelectron spectra of the nonstoichiometric $La_{2-x}Al_xO_3$ films (Al/La atomic ratio ∼0.35 to 0.4) on the Si,

Table I. Quantitative (×10^{15} #/cm²) and relative areal density of each element (in parenthesis).

		La	Si	Al	O	O/[1.5(Al + La) + 2Si]
As-deposited	$LaAlO_3$ layer except interface layer	5.22 (1)	0	5.29 (1.01)	13.55 (2.60)	0.86
	Total	5.89 (1)	1.35 (0.23)	5.97 (1.01)	15.95 (2.71)	0.78
800 °C RTA	Al rich	2.64 (1)	0.64 (0.24)	3.84 (1.45)	9.2 (3.48)	0.84
	Al deficient	3.26 (1)	4.4 (1.35)	1.98 (0.61)	15.8 (4.85)	0.95
	Total	5.9 (1)	5.04 (0.85)	5.82 (0.99)	25.0 (4.24)	0.9
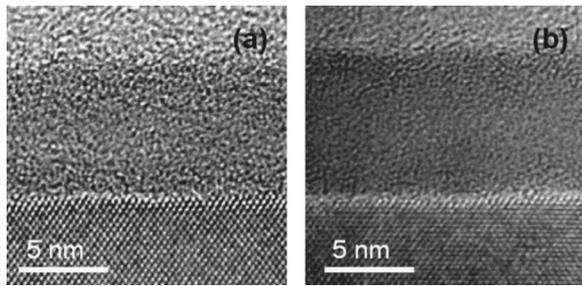
Figure 2. Cross-sectional HRTEM images of the (a) as-grown and (b) annealed LaAlO$_3$ film on Si substrate.

Figure 4. Al-to-La peak area ratios depending on the take-off angle of photoelectrons in (a) stoichiometric LaAlO$_3$ films on Si substrate and (b) nonstoichiometric LaAlO$_3$ films on various substrates.

Si$_3$N$_4$/Si, and Ru/SiO$_2$/Si substrates. Si diffusion into the film layer was suppressed in the cases of Si$_3$N$_4$/Si and Ru/SiO$_2$/Si substrates. Diffusion in the opposite direction of the Al and La atoms were also observed in the annealed nonstoichiometric La$_{2-x}$Al$_x$O$_3$/Si system. However, there was no atomic diffusion observed for the cases where La$_{2-x}$Al$_x$O$_3$ films had been deposited on the Si$_3$N$_4$/Si and Ru/SiO$_2$/Si substrates after PDA. Interestingly, the Al/La ratio was relatively constant irrespective of sin θ, suggesting that there was no counter diffusion of Al and La in these cases, even after PDA. Figure 4 also suggests that the atomic diffusion in LaAlO$_3$ films on a Si substrate has no relationship with the La/Al ratio and does not originate from the nonstoichiometry of LaAlO$_3$ films. If the atomic diffusion originated from phase separation into La$_2$O$_3$, La$_{33}$Al$_7$O$_{60}$, LaAlO$_3$, and LaAl$_{11}$O$_{18}$ phase,[14] which could be induced by the cation nonstoichiometry of La$_{2-x}$Al$_x$O$_3$ film, it should have been observed in the Al-deficient LaAlO$_3$ film on a Ru and Si$_3$N$_4$ layer. However, atomic diffusion was not observed in the Al-deficient (Fig. 4b) or -rich (not shown) LaAlO$_3$ films. Therefore, it was concluded that both Al and La diffusion are induced by Si diffusion into the LaAlO$_3$ film.

La$_2$O$_3$ films react with a Si substrate and easily form a La-silicate layer during annealing at temperatures as low as 400°C,[15] while Al-silicate films are formed at relatively high temperatures. Moreover, Al atoms are more suitable for being substituted by Si atoms than La atoms due to their similar atomic size. Therefore, Al
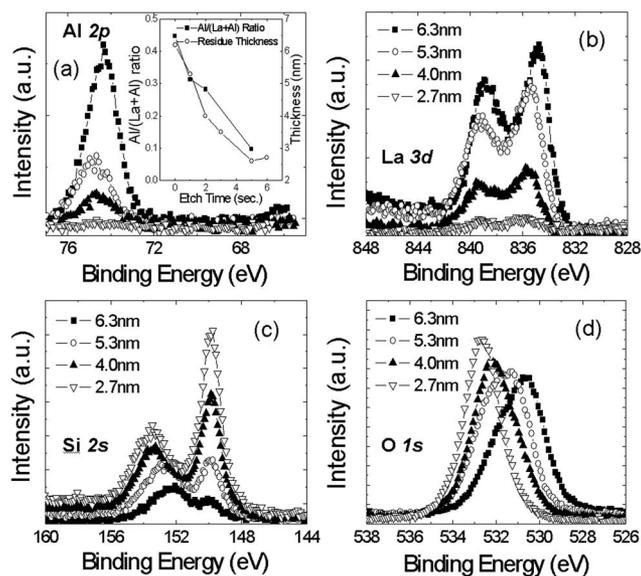
atoms, which do not participate in silicate formation during annealing, diffuse to the film surface and La atoms diffuse into the film bulk to form a La-silicate layer.

Figure 5a shows the Si 2s spectra of annealed LaAl$_x$O$_y$ films with various Al concentrations. The silicate peak (BE ≈ 152–153 eV) intensity was lower for the LaAl$_x$O$_y$ films with a higher Al concentration because the Al–O bonds are effective in suppressing Si diffusion from the substrate and reactive gases, such as water or oxygen, from residual gas in the annealing chamber.[11] Figure 5b shows the Al/(La + Al) peak area ratios as a function of the take-off angle in annealed LaAl$_x$O$_y$ films. The Al/(Al + La) ratio increased from 0.4 to 0.51 in the annealed La$_{0.65}$Al$_{0.35}$O$_{1.5}$ film and from 0.7 to 0.73 in the annealed La$_{0.32}$Al$_{0.68}$O$_{1.5}$ film when the take-off angle was decreased from 90 to 30° (sin θ of 1 and 0.5). The difference between the Al concentration at low and high take-off angles decreased from 0.11 to 0.03 as the Al content was increased from 0.35 to 0.68. This suggests that fewer Al atoms diffuse to the film surface in the films with higher Al concentration. Figures 5a and b show that a higher Al concentration results in less La-silicate layer formation and Si diffusion, which in turn reduces the counter diffusion of Al and La atoms during PDA.

It was found that atomic diffusion in LaAlO$_3$ films by PDA did not show any qualitative difference depending on the ALD temperature (176–380°C). It was also confirmed that the same diffusion behavior was observed from the LaAlO$_3$ film deposited using an electron-beam evaporation method (data not shown). It was also found that a thicker film (~9 nm, data not shown) showed less Al and La diffusion than a thinner film (~6 nm). Therefore, it appears that the counter diffusion of Al and La in a LaAlO$_3$ film is a generic property irrespective of the deposition method (e.g., ALD and *e*-beam evaporation) as long as Si diffusion is not suppressed.

In summary, the annealing effect of LaAlO$_3$ films deposited on a Si substrate was investigated. The diffusion of Si atoms from the substrate induces silicate layer formation. Because La$_2$O$_3$ reacts more easily with Si than Al$_2$O$_3$,[1,2,6,16] the Si-rich La-silicate and Al-deficient LaAl$_x$Si$_y$O$_z$ layer was formed on a few monolayers of

Figure 3. (a) Al to (La + Al) peak area ratios and residue thickness, and (b) Al 2p, (c) La 3d, (d) Si 2s, and (e) O 1s spectra before and after etching of the annealed LaAlO$_3$ films for each etch time.
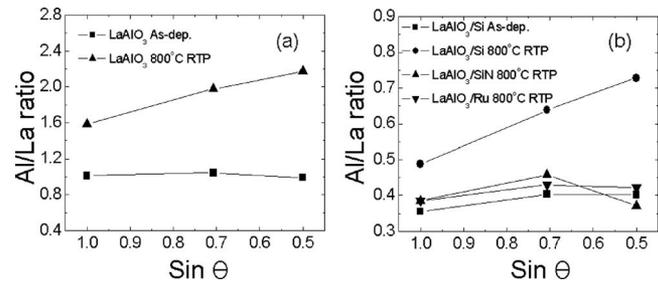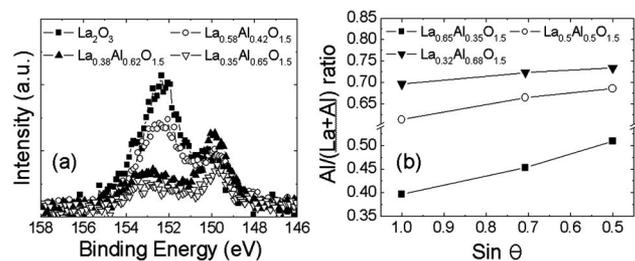

Figure 5. (a) Si 2s spectra and (b) Al-to-(La + Al) peak area ratios depending on the take-off angle of annealed LaAl$_x$O$_y$ films at various Al concentrations.

SiO_2. Al atoms, which do not participate in silicate formation during annealing, migrate toward the film surface. At the same time, La atoms migrate to the interface to form a silicate layer, which results in nonhomogeneous films. The diffusion of Al and La atoms originated from Si diffusion from the substrate. Therefore, it is essential to suppress Si diffusion from the substrate in order to preserve the uniform $LaAlO_3$ films during PDA.

References

1. X. L. Li, W. F. Xiang, H. B. Lu, and Z. H. Mai, *J. Appl. Phys.*, **97**, 124104 (2005).
2. A. D. Li, Q. Y. Shao, H. Q. Ling, J. B. Cheng, D. Wu, Z. G. Liu, N. B. Ming, C. Wang, H. W. Zhou, and B. Y. Nguyen, *Appl. Phys. Lett.*, **83**, 3540 (2003).
3. D. O. Klenov, D. G. Schlom, H. Li, and S. Stemmer, *Jpn. J. Appl. Phys., Part 2*, **44**, L617 (2005).
4. L. F. Edge, D. G. Schlom, R. T. Brewer, Y. J. Chabal, J. R. Williams, S. A. Chambers, C. Hinkle, G. Lucovsky, Y. Yang, S. Stemmer, et al., *Appl. Phys. Lett.*, **84**, 4629 (2004).
5. B. E. Park and H. Ishiwara, *Appl. Phys. Lett.*, **82**, 1197 (2003).
6. T. Busani and R. A. B. Devine, *Mater. Res. Soc. Symp. Proc.*, **786**, E6.12.1 (2004).
7. K. P. Bastos, L. Salvador, C. Krug, V. Edon, M. C. Hugon, B. Agius, and I. J. R. Baumvol, *Electrochem. Solid-State Lett.*, **10**, G69 (2007).
8. M. Hasan, M. S. Jo, M. S. Rahman, H. Choi, S. Heo, and H. Hwang, *Electrochem. Solid-State Lett.*, **9**, F77 (2006).
9. D. H. Triyoso, H. Li, R. I. Hegde, Z. Yu, K. Moore, J. Grant, B. E. White, Jr., and P. J. Tobin, *J. Vac. Sci. Technol. B*, **23**, 2480 (2005).
10. D. Eom, S. Y. No, H. Park, C. S. Hwang, and H. J. Kim, *Electrochem. Solid-State Lett.*, **10**, G93 (2007).
11. M. Kundu, N. Miyata, T. Nabatame, T. Horikawa, M. Ichikawa, and A. Toriumi, *Appl. Phys. Lett.*, **82**, 3442 (2003).
12. L. C. Feldman and J. W. Mayer, *Fundamentals of Surface and Thin Film Analysis*, p. 225, North-Holland, New York (1986).
13. A. Besmehn, A. Scholl, E. Rije, and U. Breuer, *Appl. Surf. Sci.*, **252**, 172 (2005).
14. T. S. Key and B. Crist, Jr., *J. Am. Ceram. Soc.*, **88**, 191 (2005).
15. J. S. Jur, D. J. Lichtenwalner, and A. I. Kingon, *Appl. Phys. Lett.*, **90**, 102908 (2007).
16. C. Merckling, G. Delhaye, M. El-Kazzi, S. Gaillard, Y. Rozier, L. Rapenne, B. Chenevier, O. Marty, G. Saint-Girons, M. Gendry, et al., *Microelectron. Reliab.*, **47**, 540 (2007).